$Cu_{28}H_{20}$: A Peculiar Chiral Nanocluster with an Exposed Cu Atom and 13 Surface Hydrides

Xianhu Liu[1#], Hui Shen[1#], Yang Gao[2], Guocheng Deng[1], Hongwen Deng[1], Ying-Zi Han[1], Boon K. Teo[1]* and Nanfeng Zheng[1]*

[1] State Key Laboratory for Physical Chemistry of Solid Surfaces, Collaborative Innovation Center of Chemistry for Energy Materials, and National & Local Joint Engineering Research Center for Preparation Technology of Nanomaterials, College of Chemistry and Chemical Engineering, Xiamen University, Xiamen 361005, China. [2] Institute of Fundamental and Frontier Sciences, University of Electronic Science and Technology of China, Chengdu, Sichuan 610054, China.
*E-mail: nfzheng@xmu.edu.cn; boonkteo@xmu.edu.cn
# These authors contributed equally to this work.

Experimental

Reagents: $NH_4[S_2P(OiPr)_2]$ (dtp) and $Cu(CH_3CN)_4BF_4$ were prepared according to literature methods.[1,2] 1,3-Bis(diphenylphosphino) propane (DPPP, 98%), tetrabutylammonium hexafluorophosphate (98%) and sodium borohydride ($NaBH_4$, 99%) were purchased from Energy Chemical (Shanghai, China). n-Hexane (A.R.), dichloromethane (CH_2Cl_2, A.R.), methanol (CH_3OH, A.R.), acetone (CH_3COCH_3, A.R.), ether ($C_2H_5OC_2H_5$, A.R.), ethanol (C_2H_5OH, A.R.) and acetonitrile (CH_3CN, A.R.) were purchased from Sinopharm Chemical Reagent Co. Ltd. (Shanghai, China). Water utilized in all tests was ultrapure. All other reagents were used as received without further purification.

Synthesis of $[Cu_{28}H_{20}(S_2P(OiPr)_2)_9]^-$: $Cu(CH_3CN)_4BF_4$ (315mg, 1 mmol), $NH_4[S_2P(OiPr)_2]$ (90 mg, 0.39 mmol), DPPP (150mg, 0.36 mmol) and tetrabutylammonium hexafluorophosphate (190 mg, 0.49 mol) were added to a mixed solution of CH_2Cl_2 (30 mL), methanol (10 mL) and acetonitrile (5 mL). After stirring for 15 min, $NaBH_4$ (115mg, 3 mmol) in C_2H_5OH (3.5 mL) was added dropwise. The mixture was stirred for 4h and dried by rotary evaporator. Then, methanol (20 mL) was added to precipitate the crude product. The crude product was washed with methanol for three times. Then, acetone (20 mL) was added to dissolve the targeted product. The solution was

centrifuged at 14000 rpm for 10 min and concentrated to about 4 mL. After that, the solution was subjected to diffusion of n-hexane under 4 °C. Faint yellow plate-like crystals were obtained after one week (27 % yield based on Cu). $Cu(DPPP)_2[Cu_{28}H_{20}(S_2P(OiPr)_2)_9]$, Elemental Anal. Theoretical: C, 28.13; H, 4.30; S, 12.50 Found: C, 28.46; H, 4.15; S, 12.23.

Characterization

UV-vis spectra were recorded using a UV-2550 Spectrophotometer (Shimadzu, Japan). Negative-ion electrospray ionization mass spectra (ESI-MS) were taken on a time-of-flight mass spectrometer (Agilent 6224, USA). The samples dissolved in acetone were directly infused at a flow rate of 1.2 mL/h by a syringe pump. Typical parameters used for the measurements were as follows: capillary voltage: 4.0 kV; drying gas temp: 150 °C; drying gas flow: 4 L/min; nebulizer pressure: 20 psi. ^{1}H NMR and ^{31}P NMR spectra were performed at room temperature on an AVANCE III 600 MHz spectrometer (Bruker, Germany). ^{2}H NMR spectra were collected at room temperature on AVANCE III 850 MHz spectrometer (Bruker, Germany). All NMR data were processed on MestReNova software.

X-ray single-crystal analysis: The diffraction data of the single crystal was collected on a Rigaku Oxford Diffraction system X-ray single-crystal diffractometer using Cu K_α (λ= 1.5418 Å) at 100 K. The data were processed using CrysAlisPro.[3] The structure was solved and refined using Full-matrix least-squares based on F^2 using ShelXT[4], ShelXL[5] in Olex2[6] and Shelxle.[7] Detailed crystal data and structure refinements for the nanocluster are given in **Table S6**. The CCDC number is 2119530.

Computational Method

In this study, the quantum chemical computations were performed at the density functional theory levels in Gaussian 09 software.[8] The Becke-3-Lee-Yang-Parr (B3LYP) functional[9,10] with empirical dispersion corrections, B3LYP(D3), was used to optimize the $[Cu(DPPP)_2]^+[Cu_{28}H_{20}(S_2P(OiPr)_2)_9]^-$ structure reported in this paper. Small-core relativistic effective core potentials (RECP, including 10 core electrons) with the (8s7p6d2f1g)/[6s5p3d2f1g] valence basis set was used for Cu atoms.[11,12] The double-ζ basis set [6-31G(d,p)] was used for C, O, P, S, and H atoms.[13-18] The initial structure was derived from the experimentally obtained crystal structure, based on which we have performed constrained optimization. That is, only 20 H and 28

Cu atoms were allowed to move, while all other atoms were fixed. The reason for the constrained optimization is that the $[Cu(DPPP)_2]^+[Cu_{28}H_{20}(S_2P(OiPr)_2)_9]^-$ structure is very large, it is basically impossible to fully optimize the entire structure globally. Furthermore, the crystal structure is of such high quality that the positions of the non-hydrogen atoms can be deemed as accurate that can be fixed. The DFT calculation was used to authenticate the 20 hydride positions.

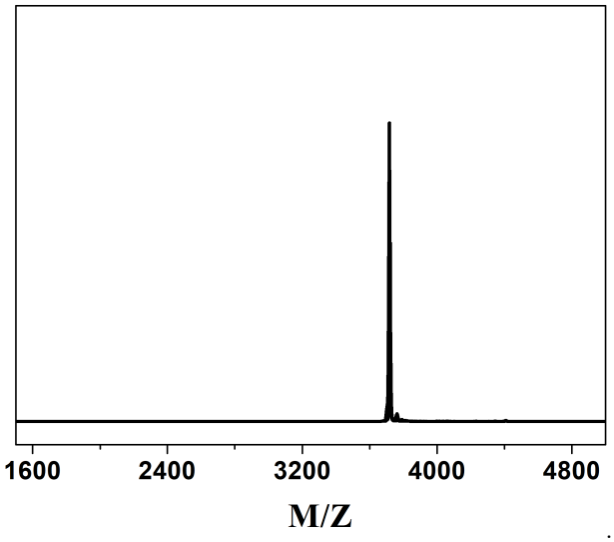

Fig S1. ESI mass spectrum of $Cu_{28}H_{20}$.

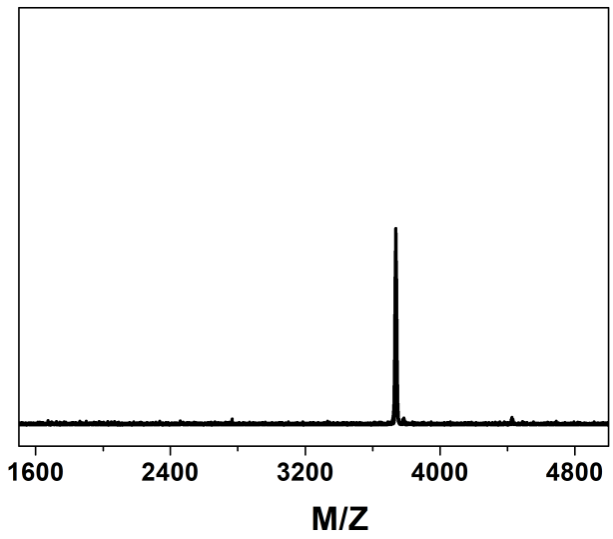

Fig S2. ESI mass spectrum of $Cu_{28}D_{20}$.

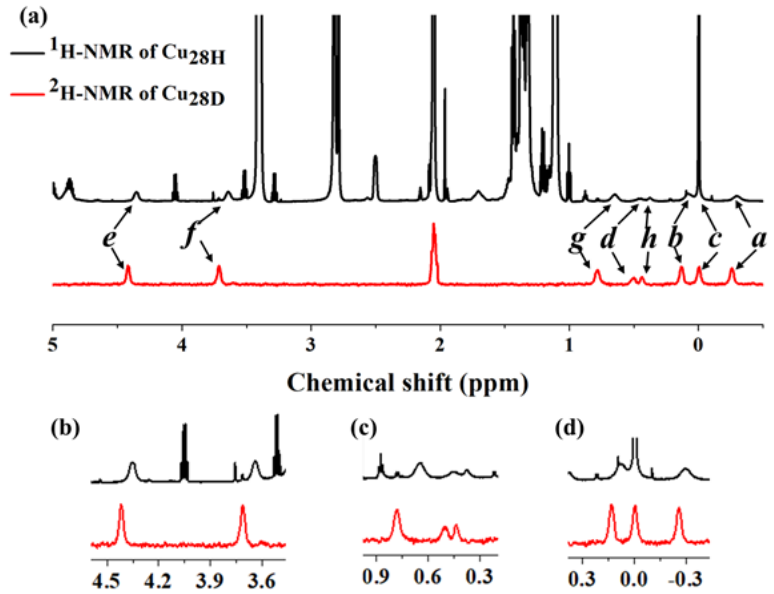

Fig S3. (a) ^{1}H-NMR spectrum of $Cu_{28}H_{20}$ in CD_3COCD_3 and ^{2}H-NMR spectrum of $Cu_{28}D_{20}$ in acetone with tetramethylsilane (TMS) and solvent residual signals as references. (b), (c), (d) The enlarged spectra of (a).

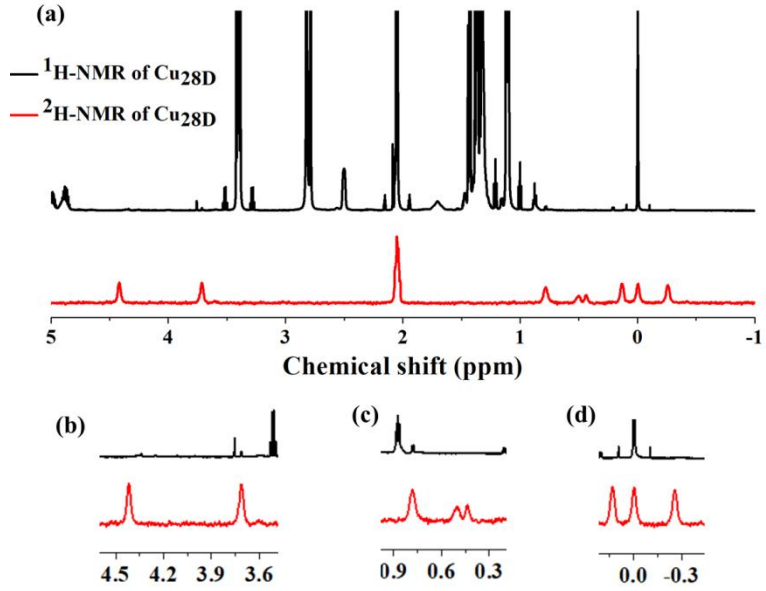

Fig S4. (a) ^{1}H-NMR spectrum of $Cu_{28}D_{20}$ in CD_3COCD_3 and ^{2}H-NMR spectrum of $Cu_{28}D_{20}$ in acetone with tetramethylsilane (TMS) and solvent residual signals as references. (b), (c), (d) The enlarged spectra of (a).

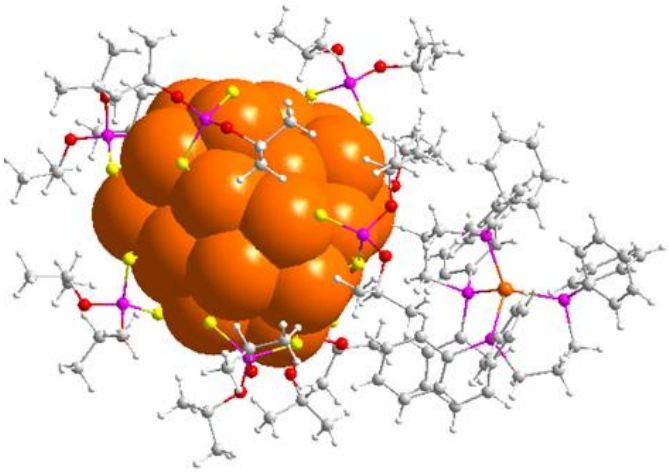

Fig S5. Full structure of $Cu_{28}H_{20}$. Atom colors: orange = Cu atoms; pink = P; yellow= S; red= oxygen; gray= carbon; white =hydrogen.

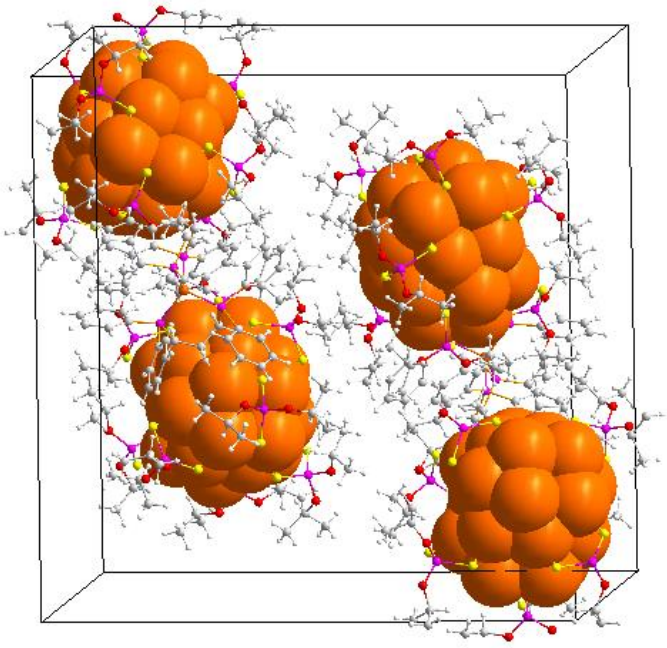

Fig S6. The packing structure of $Cu_{28}H_{20}$ in the unit cell. Atom colors: orange = Cu atoms; pink = P; yellow= S; red= oxygen; gray= carbon; white =hydrogen.

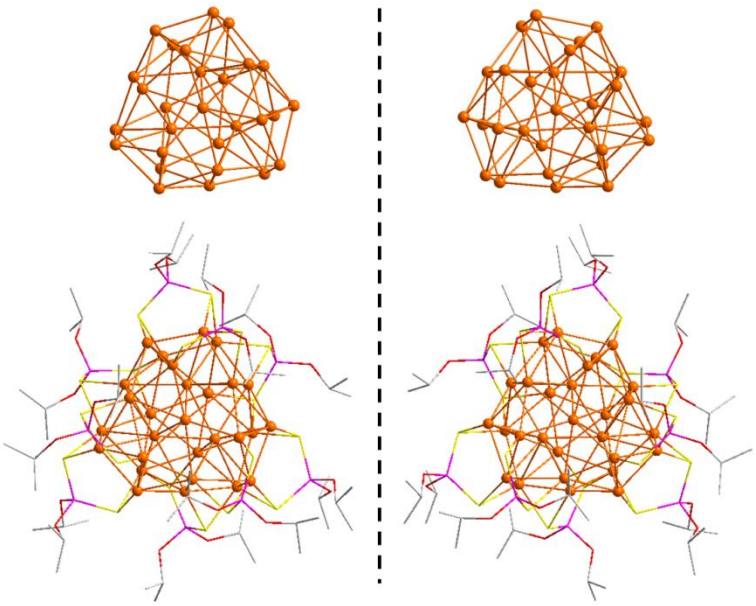

Fig S7. Representations of the two enantiomers of $Cu_{28}H_{20}$ from core to surface in the unit cell. Atom colors: orange = Cu atoms; pink = P; yellow= S; red= oxygen; gray= carbon. All hydrogen atoms are omitted for clarity.

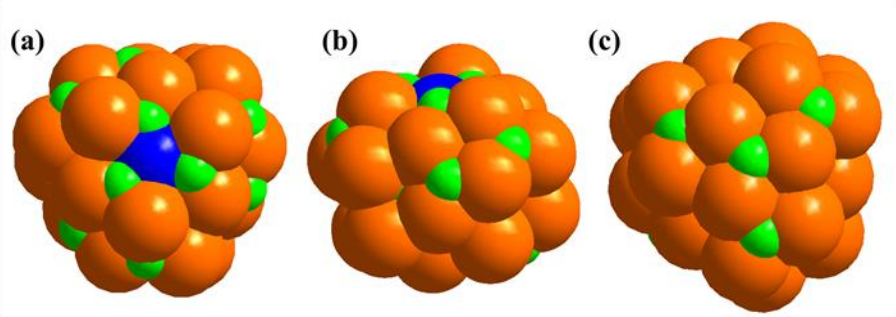

Fig S8. Space filling model of the $Cu_{28}H_{20}$ core: (a) The view along the threefold axis. (b) The view perpendicular to the threefold axis. (c) The view in the opposite direction of (a). Atom colors: orange = Cu atoms of Cu_{24} shell; blue = Cu atoms of Cu_4 core; green = H. All dtp ligands are omitted for clarity.

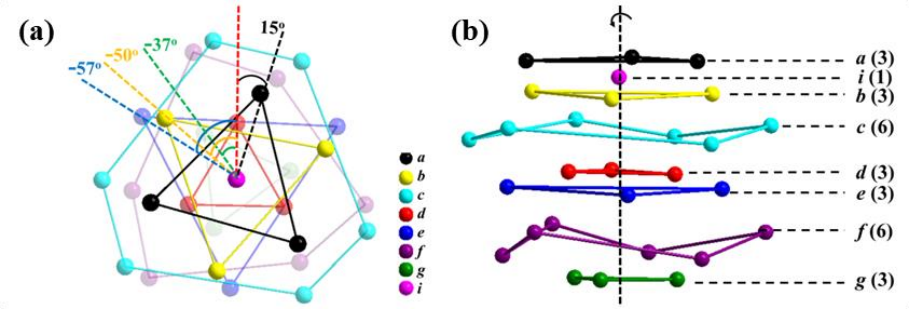

Fig S9. The view down the idealized (noncrystallographic) threefold axis (a) and a layer-by-layer representation (b) of the 28 Cu atoms in $Cu_{28}H_{20}$. The numbers of copper atoms in the corresponding layers are presented in the parentheses.

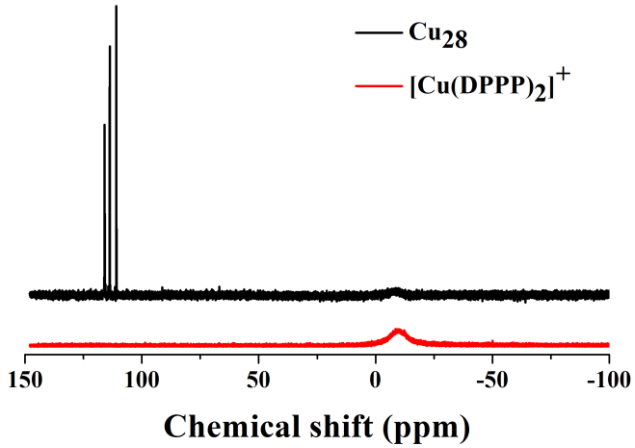

Fig S10. ^{31}P NMR spectra of $Cu_{28}H_{20}$ and $Cu(DPPP)_2$.

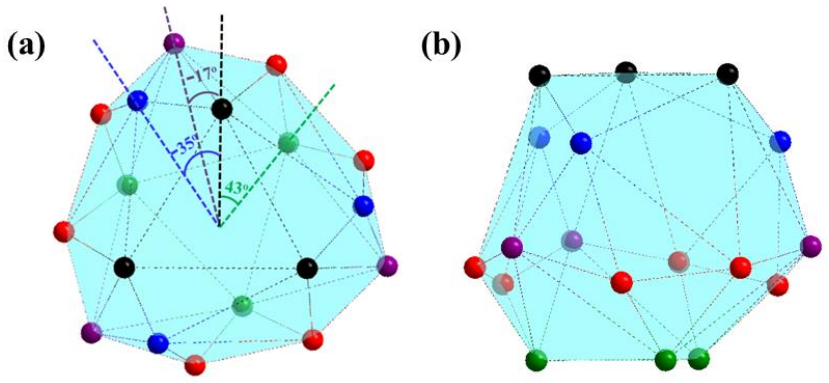

Fig S11. Top view (a) and side view (b) of 18 S atoms in $Cu_{28}H_{20}$.

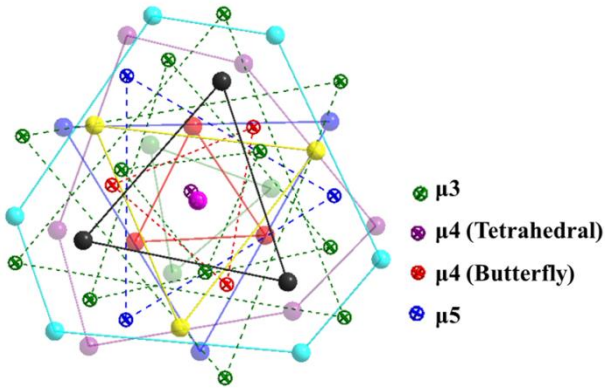

Fig S12. The view down the threefold axis of the 28 Cu atoms (solid spheres) and 20 hydrides (hollow spheres) in $Cu_{28}H_{20}$.

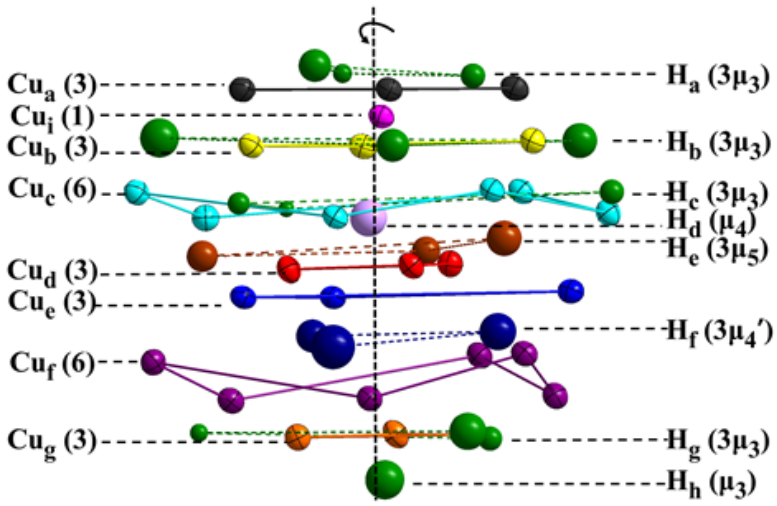

Fig S13. Layer-by-layer representation of the **$Cu_{28}H_{20}$** cluster (all *dtp* ligands are omitted for clarity). The numbers of the copper atoms (left) and hydrides (right) in the respective layers are in parentheses. Anisotropic thermal ellipsoids of the 28 copper atoms and isotropic thermal spheres of the 20 hydride atoms were set at 50% and 30% probabilities, respectively.

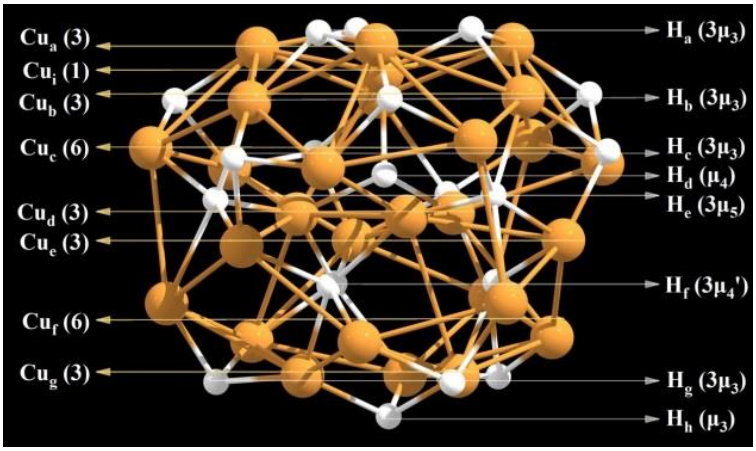

Fig S14. DFT derived $Cu_{28}H_{20}$ core of the anionic $[Cu_{28}H_{20}(S_2P(OiPr)_2)_9]^-$ cluster (all *dtp* ligands are omitted for clarity). The numbers of the copper atoms (left) and hydrides (right) in the respective layers shown in Fig. S13 are in parentheses.

Table S1. The distances (range and average) between the layers (Fig. S9(b)) and the bond lengths of Cu-Cu between the layers of $Cu_{28}H_{20}$ metal framework as determined by SC-XRD.

The distances between the layers(Å)	**The bond lengths of Cu-Cu between the layers (Å)**	**The distances of Cu-Cu within the layers (Å)**
a-*b*: 0.888	*a*-*b*: 2.5688 [a] (8)-2.9394(8) 2.7389(8)	*a*: 4.3253(8)-4.3861(8) 4.3625(8)
b-*c*: 1.149	*b*-*c*: 2.6730(8)-2.8124(8) 2.7472(8)	*b*: 4.5644(8)-4.6290(8) 4.6072(8)
c-*d*: 0.8082	*c*-*d*: 2.6713(8)-2.7645(8) 2.7085(8)	*c*: 2.5614(8)-2.6082(8), 5.0675(9)-5.1580(8) 2.5819(8), 5.1231(8)
d-*e*: 0.4673	*d*-*e*: 2.6810(8)-2.8780(8) 2.7835(8)	*d*: 2.6820(8)-2.7169(8) 2.7007(8)
e-*f*: 0.9938	*e*-*f*: 2.5234(8)-2.7121(8) 2.6155(8)	*e*: 5.4551(8)-5.5260(8) 5.4877(8)
f-*g*: 1.1275	*f*-*g*: 2.6164(8)-2.7089(8) 2.6539(8)	*f*: 2.5632(9)-2.5917(8), 4.3386(8)-4.3989(8) 2.5729(8), 4.3588(8)
		g: 2.6703(8)-2.7080(8) 2.6925(8)

[a] (8): the number in the parentheses is esd value.

Table S2. Selected bond lengths (range and average) of $Cu_{28}H_{20}$ as determined by SC-XRD.

Bond	X-ray
[a]Cu_c-Cu_c	2.6820 [e] (8)-2.8884(8) 2.7834(8)
Cu_c-[b]Cu_p	2.5484(9)-2.7720(8) 2.6934(8)
Cu_p-Cu_p	2.5234(8)-2.9394(8) 2.6889(8)
Cu_p-S(μ_1)	2.3153(13)-2.3506(13) 2.3346(13)
Cu_p-S(μ_2)	2.3082(12)-2.4782(11) 2.3739(12)
Cu_p-H(μ_3)	1.50(6)-1.89(6) 1.70(5)
Cu-[c]H(μ_4-s)	1.63 (6) – 2.07 (6) 1.78 (7)
Cu-[d]H(μ_4-t)	1.58 (6) - 1.94 (6) 1.73 (6)
Cu-H(μ_5)	1.66 (5) - 2.15 (5) 1.85(6)

[a]Cu_c = Cu atoms of Cu_4 core, [b]Cu_p = Cu atoms of Cu_{24} shell, [c]H(μ_4-s) = μ_4 hydride in butterfly geometry, [d]H(μ_4-t) = μ_4 hydride in tetrahedral cavity, [e] the numbers in parentheses are esd values.

Table S3. The numbers of S-Cu-H groups attached to the Cu_nH cluster fragments (n=3, 4, 5) and the corresponding averages of Cu-H and Cu-S bond lengths as determined by SC-XRD.

Hydride	Number of neighboring S-Cu-H groups	Average Cu-S (Å) bond length	Average Cu-H (Å) bond length
H_a	2	2.3779(12)	1.71 (5)
H_b	4	2.3497(12)	1.67 (6)
H_c	3	2.3499(12)	1.71(4)
H_d	0	none	1.73 (6)
H_e	0	none	1.85(6)
H_f	0	none	1.78(7)
H_g	5	2.3917(11)	1.68 (5)
H_h	3	2.4421(11)	1.71 (7)

Table S4. The Cu-H bond lengths (individual distances, ranges, and averages) as determined by SC-XRD.

Hydrides	The bond lengths of Cu-H (Å)	The bond length ranges of Cu-H (Å)	Average Cu-H bond length (Å)
H_a	1.65 (4), 1.67 (4), 1.80 (4) 1.73 (5), 1.64 (5), 1.63 (5) 1.89 (6), 1.72 (6), 1.68 (5)	1.63 (5) - 1.89 (6)	1.71 (5)
H_b	1.74 (6), 1.79 (6), 1.50 (6) 1.63 (6), 1.64 (6), 1.65 (6) 1.60 (6), 1.73 (6), 1.72 (6)	1.50 (6) - 1.79 (6)	1.67 (6)
H_c	1.63 (5), 1.69 (5), 1.76 (5) 1.77 (4), 1.73 (5), 1.69 (4) 1.82 (4), 1.67 (4), 1.67 (4)	1.63 (5) - 1.82 (4)	1.71 (4)
H_d	1.64 (6), 1.58 (6), 1.75 (6), 1.94 (6)	1.58 (6) - 1.94 (6)	1.73 (6)
H_e	1.89 (5), 1.82 (5), 1.71 (6), 2.15 (5), 1.74 (6) 1.89 (5), 1.96 (5), 1.99 (6), 1.71 (5), 1.66 (5) 1.88 (6), 1.68 (6), 1.94 (6), 2.09 (6), 1.68 (6)	1.66 (5) - 2.15 (5)	1.85 (6)
H_f	1.76(8), 1.70(9), 1.82(8), 1.84(9) 1.70(6), 1.63(6), 1.80(6), 2.02(6) 1.65(6), 1.71(6), 1.68(5), 2.07(6)	1.63 (6) – 2.07 (6)	1.78 (7)
H_g	1.70 (5), 1.68 (5), 1.74 (5) 1.65 (4), 1.81 (4), 1.51 (4) 1.80 (6), 1.68 (6), 1.57 (6)	1.51 (4) - 1.81 (4)	1.68 (5)
H_h	1.74 (6), 1.67 (7), 1.72 (6)	1.67 (7) - 1.74 (6)	1.71 (7)

Table S5. DFT calculated Cu-H bond lengths (individual distances, ranges, and averages), for comparison with Table S4.

Hydrides	Bond lengths of Cu-H (Å)	Bond length ranges of Cu-H (Å)	Average bond length
H_a	1.679; 1.705; 1.697 1.700; 1.724; 1.664 1.702; 1.669; 1.717	1.664 ~ 1.724	1.695
H_b	1.662; 1.770; 1.661 1.789; 1.656; 1.649 1.646; 1.811; 1.654	1.646 ~ 1.811	1.700
H_c	1.689; 1.704; 1.737 1.735; 1.691; 1.698 1.696; 1.731; 1.697	1.689 ~ 1.737	1.709
H_d	1.729; 1.715; 1.717; 1.722	1.715 ~ 1.729	1.721
H_e	1.728; 1.872; 1.822; 2.311; 1.668 1.667; 1.713; 2.482; 1.765; 1.913 2.093; 1.808; 1.985; 1.754; 1.672	1.667 ~ 2.482	1.884
H_f	1.685; 2.204; 1.679; 1.756 1.714; 1.712; 1.696; 2.203 2.010; 1.664; 1.716; 1.744	1.664 ~ 2.204	1.815
H_g	1.672; 1.704; 1.741 1.724; 1.660; 1.758 1.715; 1.664; 1.747	1.660 ~ 1.758	1.709
H_h	1.678; 1.689; 1.688	1.678 ~ 1.689	1.685

Table S6. Validation of empirical rules for the reported copper hydride clusters characterized by neutron diffraction.

Copper hydride clusters	**Rule 1**	**Rule 2**	**Rule 3**	**References**
Cu_{20}	#	--	#	19
chiral Cu_{20}	#	#	#	20
Cu_{28}	#	--	--	21
Cu_{30}	#	--	--	22
'#': This symbol indicates the rule is applicable in the assignment of the H nmr peaks of the corresponding cluster. '--': This symbol indicates the rule is not needed to explain the assignment of the H nmr peaks of the corresponding cluster.				

References

1. Gianini, M.; Caseri, W. R.; Gramlich, V.; Suter, U. W., *Inorg. Chim. Acta.* **2000**, *299*, 199-208.
2. Ghosh, A.; Huang, R.-W.; Alamer, B.; Abou-Hamad, E.; Hedhili, M. N.; Mohammed, O. F.; Bakr, O. M., *ACS Mater. Lett.* **2019**, *1*, 297-302.
3. CrysAlisPro Version 1.171.35.19. (2013). Agilent Technologies Inc. Oxfordshire, OX5 1QU, UK.
4. G. M. Sheldrick, *Acta Cryst. A* **2015**, *71*, 3-8.
5. G. M. Sheldrick, *Acta Cryst. A* **2008**, *64*, 112-122.
6. O. V. Dolomanov, L. J. Bourhis, R. J. Gildea, J. A. K. Howard, H. Puschmann, *J. Appl. Cryst.* **2009**, *42*, 339-341.
7. C. B. Hubschle, G. M. Sheldrick, B. Dittrich, *J. Appl. Cryst.* **2011**, *44*, 1281-1284.
8. Frisch, M. J.; Trucks G. W.; Schlegel H. B.; Scuseria G. E, *et. al*. Gaussian 09 Revision D.01, Wallingford CT. **2013**,
9. Becke, A. D. Density-Functional Thermochemistry .3. The Role Of Exact Exchange. *J Chem Phys*. **1993**, 98, 5648-5652.
10. Lee, C. T.; Yang W. T.; Parr R. G. Development Of the Colle-Salvetti Correlation-Energy Formula into a Functional Of the Electron-Density. *Phys Rev B*. **1988**, 37, 785-789.
11. Dolg, M.; Wedig U.; Stoll H.; Preuss H. Energy‐adjustedabinitiopseudopotentials for the first row transition elements. *J Chem Phys*. **1987**, 86, 866-872.
12. Martin, J. M. L.; Sundermann A. Correlation consistent valence basis sets for use with the Stuttgart–Dresden–Bonn relativistic effective core potentials: The atoms Ga–Kr and In–Xe. *J Chem Phys*. **2001**, 114, 3408-3420.
13. Binkley, J. S.; Pople J. A.; Hehre W. J. Self-consistent molecular orbital methods. 21. Small split-valence basis sets for first-row elements. *J Am Chem Soc*. **1980**, 102, 939-947.
14. Gordon, M. S.; Binkley J. S.; Pople J. A.; Pietro W. J.; Hehre W. J. Self-consistent molecular-orbital methods. 22. Small split-valence basis sets for second-row elements. *J Am Chem Soc*. **1982**, 104, 2797-2803.
15. Pietro, W. J.; Francl M. M.; Hehre W. J.; DeFrees D. J.; Pople J. A.; Binkley J. S. Self-consistent molecular orbital methods. 24. Supplemented small split-valence basis sets for second-row elements. *J Am Chem Soc*. **1982**, 104, 5039-5048.
16. Dobbs, K. D.; Hehre W. J. Molecular orbital theory of the properties of inorganic and organometallic compounds 4. Extended basis sets for third-and fourth-row, main-group elements. *J Comp Chem*. **1986**, 7, 359-378.
17. Dobbs, K. D.; Hehre W. J. Molecular orbital theory of the properties of inorganic and organometallic compounds 5. Extended basis sets for first-row transition metals. *J Comp*

Chem. **1987**, 8, 861-879.

18. Dobbs, K. D.; Hehre W. J. Molecular orbital theory of the properties of inorganic and organometallic compounds. 6. Extended basis sets for second-row transition metals. *J Comp Chem*. **1987**, 8, 880-893.
19. R. S. Dhayal, J.-H. Liao, Y.-R. Lin, P.-K. Liao, S. Kahlal, J.-Y. Saillard and C. W. Liu, *J. Am. Chem. Soc.*, 2013, **135**, 4704-4707.
20. R. S. Dhayal, J.-H. Liao, X. Wang, Y.-C. Liu, M.-H. Chiang, S. Kahlal, J.-Y. Saillard and C. W. Liu, *Angew. Chem. Int. Ed.*, 2015, **54**, 13604-13608.
21. A. J. Edwards, R. S. Dhayal, P.-K. Liao, J.-H. Liao, M.-H. Chiang, R. O. Piltz, S. Kahlal, J.-Y. Saillard and C. W. Liu, *Angew. Chem. Int. Ed.*, 2014, **53**, 7214-7218.
22. S. K. Barik, S.-C. Huo, C.-Y. Wu, T.-H. Chiu, J.-H. Liao, X. Wang, S. Kahlal, J.-Y. Saillard and C. W. Liu, *Chem. Eur. J.*, 2020, **26**, 10471-10479.